processes

MDPI

Article

Comparison of Medium-Pressure UV/Peracetic Acid to Remove Three Typical Refractory Contaminants of Textile Wastewater

Yanping Zhu [1], Yuxuan Cao [1], Shihu Shu [1], Pengjin Zhu [2], Dongfang Wang [1], He Xu [1] and Dongqing Cai [1,*]

[1] College of Environmental Science and Engineering, Donghua University, Shanghai 201620, China
[2] Guangxi Subtropical Crops Research Institute, Nanning 530000, China
* Correspondence: dqcai@dhu.edu.cn

Abstract: In this work, the performance of medium-pressure UV/peracetic acid (MPUV/PAA/H_2O_2) was explored on removing reactive black 5 (RB5), aniline (ANL), and polyvinyl alcohol (PVA), three typical refractory contaminants in printing and dyeing wastewater, compared with MPUV/H_2O_2. MPUV/PAA/H_2O_2 showed 75.0, 44.9, and 57.7% removals of RB5, ANL, and PVA, respectively, within 5 min. The removal of RB5 increased from 68.98 to 91.2%, with pH increasing from 6 to 9, while the removals of ANL and PVA were much less pH-dependent. Quenching experiment results indicated that UV photolysis and radical (i.e., •OH and R-C•) oxidation contributed to RB5 removal, while PAA showed high activity in the oxidation of ANL. For PVA, •OH oxidation and UV photolysis were likely the main mechanisms. The coexisting natural organic matter had a negative effect on the degradation of RB5 and PVA. In addition, MPUV/PAA/H_2O_2 could effectively degrade those pollutants without increasing the toxicity. This work provides a theoretical reference for the utilization of MPUV/PAA/H_2O_2 in removing structurally diverse refractory contaminants from printing and dyeing wastewater.

Keywords: MPUV/PAA; reactive blank 5; aniline; polyvinyl alcohol; advanced oxidation

check for updates

Citation: Zhu, Y.; Cao, Y.; Shu, S.; Zhu, P.; Wang, D.; Xu, H.; Cai, D. Comparison of Medium-Pressure UV/Peracetic Acid to Remove Three Typical Refractory Contaminants of Textile Wastewater. *Processes* **2023**, *11*, 1183. https://doi.org/10.3390/pr11041183

Academic Editor: Florian Ion Tiberiu Petrescu

Received: 23 March 2023
Revised: 6 April 2023
Accepted: 10 April 2023
Published: 12 April 2023

1. Introduction

As a country with a large textile industry, China's printing and dyeing wastewater emissions are growing [1]. As shown in the 2015 Annual Report on Environmental Statistics, printing and dyeing wastewater emissions ranked in the top 4 of the 41 industrial sectors surveyed and reported, at 1.84 billion tons. Printing and dyeing wastewater mainly includes wastewater such as de-sizing, scouring, bleaching, and mercerized wastewater. The printing and dyeing wastewater contains various organic contaminants such as dyes, pastes, binders, dispersants, surfactants, and volatile organic compounds [2]. This type of wastewater poses a serious threat to the environment and has toxic effects on organisms if discharged directly into water bodies [3]. For a long time, printing and dyeing wastewater has been a difficult area in industrial wastewater treatment due to its high color and high concentrations of non-degradable organic matter. The printing and dyeing wastewater is generally discharged to urban wastewater treatment plants (WWTP) after on-site treatment in the factory, and then treated through conventional bio-chemical processes. Until now, different methods have been utilized for the removal of printing and dyeing wastewater, such as adsorption [4,5], precipitation [6,7], coagulation–flocculation [8,9], chemical oxidation [10–12], biological processes [13,14], and membrane filtration technology [15–17].

The advanced oxidation process (AOP) is a type of chemical oxidation and a widely used tertiary treatment process for the removal of low-level, refractory organic pollutants from the secondary effluent of textile industry wastewater. The AOP focuses on the rapid reaction of hydroxyl radicals (•OH) with organic matter using oxidants combined with catalysts, ultrasound, and photo to remove refractory organic pollutants [18]. AOPs have a higher oxidation reaction rate than conventional oxidants, and •OH can partially or

completely degrade toxic pollutants and their by-products at a high rate, such as chemicals, dyes, and pesticides. Therefore, AOP has great promise for the removal of printing and dyeing wastewater.

Reactive dyes, aniline (ANL), and polyvinyl alcohol (PVA) are three types of typical refractory pollutants in printing and dyeing wastewater and of increasing environmental concern [19]. Nevertheless, the existence of these structurally diverse refractory pollutants has caused difficulties in meeting the growing strict discharge standards. Specifically, two-thirds of the world's reactive dyes are non-degradable azo dyes, which are difficult to dispose of due to the azo bonds and polycyclic aromatic structures. Azo dyes are widely present in printing and dyeing wastewater, and reactive black 5 (RB5) is a typical non-degradable azo dye with a complex structure, thermal stability, and high solubility in water. Studies have proven its carcinogenic, teratogenic and mutagenic effects [20]. ANL, as a priority pollutant by the Environmental Protection Agency of the United States [21], is an important intermediate in the synthesis of benzidine azo dyes and a derived product during the biodegradation of azo dyes [19]. Due to its carcinogenic and mutagenic effects [22], the discharge of ANLs was forbidden in the latest 39 amended textile wastewater discharge standard (GB 4287-2012) in China [23], which greatly increased the treatment difficulty. PVA is a refractory polymer with high solubility and is widely used in the textile industry, where it is lost to printing and dyeing wastewater during the de-sizing process. The discharge of PVA can cause a lack of dissolved oxygen in the water system and the release of harmful metals in the sediment [24], thus deteriorating the water body receiver.

For decades, wastewater has mostly been disinfected using chlorine, producing disinfection by-products (DBPs) that are carcinogenic and teratogenic to humans. As a result, it is crucial to find an oxidant that could replace chlorine and produce less DBPs. Peroxyacetic acid (PAA), with a lower cost and less DBPs, is an organic disinfectant that can be used as an effective alternative for chlorinated disinfectants [25]. The PAA system is actually an equilibrium mixture of PAA, H_2O_2, and acetic acid [26], and is considered as an emerging oxidant in the advanced oxidation process (AOP) to remove organic micropollutants in water. The activation of PAA mainly included ultraviolet (UV) irradiation, ultrasound, and metal catalysis, with UV being the most commonly used activation method due to its simple, environment-friendly, and economic properties [27]. UV-catalytic oxidation is a new AOP that uses UV radiation as a source of external energy to allow oxidants to oxidize refractory organic matter, showing advantages of mild reaction conditions and a wide range of applications. The main reactions of PAA in the presence of UV irradiation are as follows:

$$CH_3COO(O)H \rightarrow CH_3C(O)O\bullet + \bullet\mathrm{OH} \quad (1)$$

UV irradiation alone achieves partial degradation of organic pollutants by breaking the chemical bonds of organic compounds. In addition, PAA itself has the potential to degrade organic micro-pollutants in water and, when combined with UV, can degrade pollutants by a variety of mechanisms: direct UV photolysis, direct oxidation, and the synergistic effect of UV and PAA (formation of radical oxidation species). Studies have shown that UV/PAA/H_2O_2 can improve the efficiency of disinfection and contaminant degradation through synergistic effects and is a promising technology for water treatment. In the UV/PAA/H_2O_2 system, abundant radicals, including •OH and R-C• (e.g., $CH_3C(O)O\bullet$, $CH_3C(O)\bullet$, and $CH_3C(O)OO\bullet$), would be generated and proved effective in the removal of diverse refractory micro-pollutants. Different from •OH, the reactivity of R-C• was selective towards structurally diverse organics, resulting in a compound-specific removal performance of UV/PAA/H_2O_2. In previous research, UV/PAA/H_2O_2 has showed comparable or even superior performance compared to UV/H_2O_2 AOP in the removal of diverse refractory micro-pollutants such as phenols and pharmaceuticals. Sharma et al. [28] demonstrated that degradation of chlorophenol congeners (4-chlorophenol, 2,4-dichlorophenol, and 2,4,6-trichlorophenol) was mediated by UV/PAA/H_2O_2. Cai et al. [29] utilized the UA/PAA/H_2O_2 system for the degradation of drugs (carbamazepine, ibuprofen, and naphthyl compounds), confirming the advantages of the system and further investigating the

degradation mechanism. In addition, the degradation kinetics and mechanism of diclofenac in UV/PAA/H_2O_2 have also been investigated, showing that the UV/PAA/H_2O_2 system is a promising method for the removal of phenols from contaminated water [30].

In terms of AOP-based textile wastewater treatment, a great many studies have reported the degradation of azo dyes, ANL, or PVA by UV/H_2O_2 systems. Araujo et al. [31] demonstrated the feasibility of degrading two azo dyes (reactive blue 214 and reactive red 243) in the UV/H_2O_2 system. Xue et al. [32] compared the degradation of ANL in both UV/H_2O_2 and UV/CaO_2 systems and found the former to be highly advantageous. In addition, another study [33] reached similar conclusions when comparing the removals of PVA by UV/H_2O_2 and UV/$S_2O_8{}^{2-}$ systems. However, the effectiveness and removal mechanism of the UV/PAA/H_2O_2 on organic pollutants in textile wastewater has rarely been studied. Therefore, there is an urgent need to evaluate its feasibility in the removal of structurally different typical pollutants from printing and dyeing wastewater.

In this study, RB5, ANL, and PVA were chosen as three typical pollutants in printing and dyeing wastewater, the removal performance of which were comparatively explored by medium-pressure (MP) UV/PAA/H_2O_2 AOP. Therein, RB5 represented aromatic compounds containing a naphthyl ring, ANL represented simple benzene-contained aromatics, and PVA represented aliphatic polymers. The influences of PAA dosage and coexisting substances (i.e., $SO_4{}^{2-}$, Cl^-, and natural organic matter) were investigated on their removal efficiency. The contributions of radicals (•OH and PAA-related R-C•), UV irradiation, and PAA oxidation under different pH conditions were discussed. Besides, the acute toxicity alteration after the treatment was evaluated. The results may provide knowledge for the application of UV/PAA/H_2O_2 AOP in printing and dyeing wastewater treatment.

2. Materials and Methods

2.1. Reagents and Materials

Hydrogen peroxide (H_2O_2, 30%), acetic acid (CH_3COOH, 99%), and ANL (C_6H_7N, 99%) were purchased from Sigma-Aldrich (Shanghai, China). RB5 ($C_{26}H_{21}N_5Na_4O_{19}S_6$), polyvinyl alcohol (PVA, $[C_2H_4O]_n$), sodium hydroxide (NaOH), potassium phosphate (K_3PO_4), dipotassium phosphate (K_2HPO_4) and monopotassium phosphate (KH_2PO_4), boric acid (H_3BO_3), potassium iodide (KI, 99%), iodine (I_2), and *tert*-butanol (TBA, $C_4H_{10}O$, 99%) were provided by Sinopharm Chemical Reagent Company (Shanghai, China). Fulvic acid (FA), phosphoric acid (H_3PO_4, 99%), and methanol (MeOH, CH_3OH, 99%) were provided by Fisher Scientific (Fair Lawn, NJ, 102 USA). N, N-Diethyl-p-phenylenediamine (DPD) was purchased from Macklin Biochemical Co., Ltd. (Shanghai, China). All chemicals were of analytical grade.

The secondary effluent from the wastewater treatment plant (Shanghai, China) was selected as real wastewater, with an initial pH of 6.8. After filtration through a 0.45 μm membrane, the dissolved organic carbon (DOC) was 4.5 mg/L. The molar ratio of PAA:H_2O_2 in the PAA solution used in this work was 1.34, freshly prepared according to Equation (2) and stored at 4 °C [34]:

$$CH_3COOH + H_2O_2 \overset{H_2SO_4}{\leftrightarrow} CH_3C(O)OOH + H_2O \quad (2)$$

2.2. Experimental Section

The target contaminant (10 mg/L) was added to 100 mL of phosphate buffer solution (10 mM, pH 7.5) and contained in a cylindrical petri dish (8 cm in diameter and 2.5 cm in depth). Then, the solution was placed under the UV lamp with a running magnetic stirrer at 200 r/min. The system was dosed with 15 mg/L of PAA solution (containing 3 mg/L of H_2O_2) and simultaneously irradiated at 25 ± 2 °C. Samples (1 mL) were withdrawn at 0, 0.5, 1, 2, 3, 4, and 5 min and immediately quenched by excessive sodium thiosulfate ($[Na_2S_2O_3]/[PAA]_0$ molar ratio > 10) for analysis. In comparison, the removal of contaminants by MPUV alone, PAA alone, and MPUV/H_2O_2 (containing 3 mg/L of H_2O_2) was also investigated. UV irradiation was performed by a UV collimated beam device,

composed of four medium-pressure UV lamps (7.5 W, Tianjin Xinjing Company, China). The lamp was preheated for at least 2 min to keep the light stable. The average irradiance was measured to be 5 mW/cm^2 by the calibrated Ocean Optics Spectro radiometer (USB4000). The influences of PAA concentration (5, 15, 30, and 50 mg/L) and pH (6, 7.5, and 9) on the removal rate of three target pollutants were also explored.

To determine the contribution of radicals, quenching tests were conducted by adding 0.1 M TBA or 0.1 M EtOH to the reaction solution before adding PAA. The effect of coexisting substances on the removal of the three target pollutants by MPUV/PAA was investigated by adding 0–2000 mg/L of inorganic anions (SO_4^{2-}, Cl^-) or 0–10 mg C/L of organic matter (using fulvic acid as a model of natural organic matter) to the working solution. All experiments were conducted at least in duplicate, and the error bars represent standard deviation.

The toxicity variation of the three pollutants was evaluated using Vibrio fischeri relevant to the treatments of MPUV alone, PAA alone, MPUV/PAA, and MPUV/H_2O_2. The effect of the quencher (Na_2SO_3) on Vibrio fischeri was also separately tested. The detected luminescence intensity was brought into Equation (2) and the final Vibrio fischeri luminescence inhibition was required to subtract the quencher inhibition.

A bioluminescent bacteria acute toxicity test was conducted via the following steps. The bacteria recovery solution was cooled at 4 °C in advance. A bottle of lyophilized bacteria was taken out from the refrigerator at −18 °C, and 3 mL of the pre-cooled bacteria recovery solution was immediately added into the lyophilized bacteria, and the bacteria lyophilized powder was gently shaken to make it quickly dissolve. The resuscitated bioluminescent bacterial suspension was stored as a reserve liquid in a 4 °C refrigerator. The osmotic pressure was adjusted in a proportion of 1 mL of each sample to 0.1 mL of osmotic pressure-regulating solution. Then, 0.5 mL of diluted bacterial solution was added to each test tube: 0.5 mL of bacterial resuscitation solution was added to the first test tube as a blank control, and 0.5 mL samples were added to the rest of the test tubes. After 15 min of reaction, luminescence intensity was successively tested:

$$IL\% = \left(\frac{I_0 - I_{5\ min}}{I_0} - I_{Na_2SO_3}\right) * 100\% \quad (3)$$

IL: The inhibitory rates of luminescence, IL%.
I_0: Luminous intensity of the negative control sample.
$I_{5\ min}$: Treated for 5 min.
$I_{Na_2SO_3}$: Luminous intensity of the quencher.

2.3. Analysis Methods

The concentration of RB5 was measured using a UV spectrophotometer (UV 1900 i, Japan) at a wavelength of 598 nm [35]. The concentration of ANL was detected via high-performance liquid chromatography (HPLC, Shimadzu LC-16, Agilent Technologies Ltd. CA, USA), equipped with a UV detector at 230 nm. HPLC analysis was carried out with the Symmetry-C18 column (5 µm, 4.6 mm × 250 mm). The mobile phase for ANL was a mixture of methanol and ultrapure water (80/20 in volume) at a flow rate of 0.8 mL/min [26]. The H_3BO_3-KI colorimetric–spectrophotometric method was used to determine the PVA concentration [36]. Standard PVA solutions (0.5 g/L) of 0, 0.05, 0.1, 0.2, 0.3, 0.4, 0.5, and 0.6 mL were added to eight volumetric flasks (25 mL) and diluted to 10 mL with water, respectively. Then, 5 mL of boric acid (4%) and 2 mL of I_2-KI (1.27 g/L I_2 and 25 g/L KI) were added to the systems. After equilibration for 5 min, the solutions were fixed to 25 mL to measure absorbance at 690 nm. The PAA stock solution was regularly calibrated using the iodine titration method and the potassium permanganate titration method [22]. The concentrations of PAA and H_2O_2 in the working solution were determined according to the DPD method [37]. Vibrio fischeri was used for toxicity testing and the luminescence intensity was measured with a portable water biotoxicity analyzer (HACH, TX131518, Ames, IA, USA) [38].

3. Results and Discussions

3.1. Removal Efficiency Assessment for Different Systems

The removal rates of RB5, ANL, and PVA by PAA/H_2O_2, MPUV alone, MPUV/PAA/H_2O_2, and MPUV/H_2O_2 were compared. As shown in Figure 1, PAA/H_2O_2 had no removal effects on RB5 and PVA, while it contributed to ANL removal of 18.25% within 5 min. Considering the reported low reactivity of H_2O_2 towards ANL [39], PAA played a key role in its removal, which was consistent with the selective oxidation of PAA to anilines [40–42]. Under the irradiation of MPUV alone, the removal rates of RB5, ANL, and PVA were 31.9, 24.4, and 38.9%, respectively, indicating the contribution of photolysis. In the MPUV/PAA/H_2O_2 system, the removal rates of RB5, ANL, and PVA were 75.0, 44.9, and 57.7% within 5 min, respectively, likely because of the radicals produced by MPUV activation of PAA and H_2O_2 [43,44]. In the MPUV/H_2O_2 system, the removal efficiency of RB5 was similar to that of the MPUV/PAA/H_2O_2 system, indicating the insignificant effect of PAA. The removal rate of ANL in the MPUV/H_2O_2 system was 15.2% lower than that of the MPUV/PAA/H_2O_2 system, likely due to the oxidation of PAA and its derived radicals [45]. Interestingly, the degradation of PVA was better in MPUV/H_2O_2 (87.87%) compared to the MPUV/PAA/H_2O_2 (57.74%) system, indicating that the coexisting PAA may react with •OH to produce R-C• with a low reactivity with PVA, according to reactions (3)–(6) [27,46]. Those results demonstrated that MPUV/PAA/H_2O_2 showed a selectivity to aromatic organics such as ANL and RB5.

$$CH_3C(O)O^- + \bullet OH \rightarrow \bullet CH_2C(O)O^- + H_2O \tag{4}$$

$$CH_3CO_3H + \bullet OH \rightarrow \bullet CH_3CO_3\bullet + H_2O \tag{5}$$

$$CH_3CO_3H + \bullet OH \rightarrow \bullet CH_3CO\bullet + H_2O \tag{6}$$

$$CH_3CO_3H + \bullet OH \rightarrow \bullet CH_3CO_2\mathrm{H}\bullet + \bullet\mathrm{OOH} \tag{7}$$

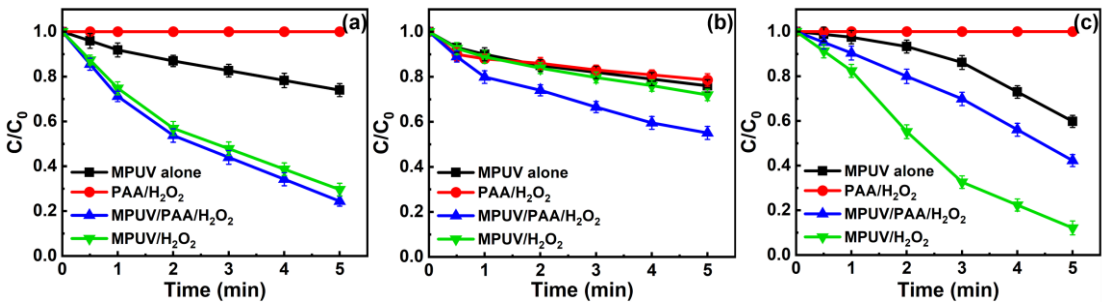

Figure 1. Effects of PAA/H_2O_2, MPUV alone, MPUV/PAA/H_2O_2, and MPUV/H_2O_2 systems on the removal of (**a**) RB5, (**b**) ANL, and (**c**) PVA. Conditions: $[PAA]_0$ = 15 mg/L, $[H_2O_2]_0$ = 3 mg/L, $[Contaminant]_0$ = 10 mg/L, UV fluence rate = 5 mW/cm^2, UV exposure time = 5 min, pH 7.5, with 10 M phosphate buffer, T = 25 ± 1 °C.

3.2. Effects of PAA Dosage and pH on Pollutants' Removal

In Figure 2a–c, as the PAA dosage increased from 5 to 50 mg/L, the removal rate of RB5 increased from 25.8 to 82.7%, which may be mainly attributed to the increased amounts of radicals produced by MPUV-activated H_2O_2 [47,48]. As for ANL, the removal rate showed an increasing trend as PAA dosage increased (from 5 to 30 mg/L). However, when the PAA dosage was 50 mg/L, the removal rate decreased compared to 30 mg/L. As for ANL, with the increasing PAA dosage, the removal rate initially increased (from 5 to 30 mg/L) and then (from 30 to 50 mg/L) decreased, reaching the maximum removal rate of 64.84%. This was probably because the overuse of PAA could consume a part of the

radicals [49]. The PAA dosage variation exhibited an insignificant influence on the removal of PVA, indicating that the acetic acid, PAA, and H_2O_2 may consume radicals in the system, according to reactions (3)–(7).

$$HOOH + HO\bullet \rightarrow HOO\bullet + H_2O \quad (8)$$

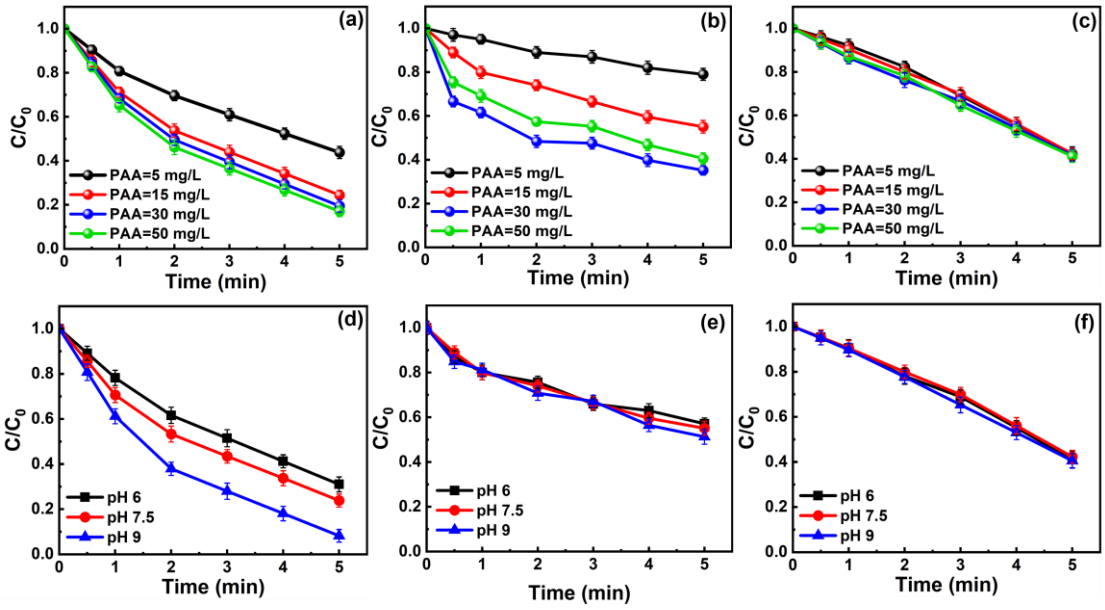

Figure 2. Effect of PAA dosage and pH on the removal of (**a**,**d**) RB5, (**b**,**e**) ANL, and (**c**,**f**) PVA in the MPUV/PAA/H_2O_2 system. Conditions: $[\text{Contaminant}]_0$ = 10 mg/L, $[\text{PAA}]_0$ = 15 mg/L, $[H_2O_2]_0$ = 3 mg/L, UV fluence rate = 5 mW/cm^2, UV exposure time = 5 min, T = 25 ± 1 °C.

As displayed in Figure 2d–f, with the increasing pH, the removal rate of RB5 increased from 68.98 to 91.2% in 5 min, while the removal rates of ANL and PVA were less pH-dependent, in the ranges of 42.9–48.7% and 57–58%, respectively. The higher removal of RB5 under the alkaline condition was in consistent with the reported work using photolytic or ozone AOP systems [50,51]. The minor effect of pH on the removal of ANL and PVA may be related to combined contributions of PAA/radicals' oxidation and photolysis.

3.3. Radicals' Contribution in the MPUV/PAA/H_2O_2 System

Quenching experiments were carried out to investigate the contribution of radicals in the MPUV/PAA/H_2O_2 system at different pH levels. As illustrated in Figure 3, the removal of RB5 in the MPUV/PAA/H_2O_2 system increased from 68.9 to 76.1% and 91.8%, with a pH rise from 6 to 7.5 and 9. Meanwhile, the removal rates under UV irradiation were 16.1%, 31.9%, and 39.4% at pH 6, 7.5, and 9, corresponding to relative contributions of UV photolysis of 23.4%, 41.9%, and 42.9%. With the addition of TBA, the removal rates of RB5 significantly decreased to 33.64, 42.13, and 58.36% at pH 6, 7.5, and 9, respectively. The addition of MeOH resulted in a further decrease of RB5's removal to 18%, 19.4%, and 39.8%, respectively. Herein, TBA was used to quench •OH ($k_{\bullet OH/TBA}$ = (3.8–7.6) × 10^8 $M^{-1}s^{-1}$) [52], and MeOH for both •OH ($k_{\bullet OH/MeOH}$ = 9.16 × 10^9 $M^{-1}s^{-1}$) [53] and R-C• [54]. The results indicated that UV photolysis and oxidation of radicals including •OH and R-C• contributed to the degradation of RB5.

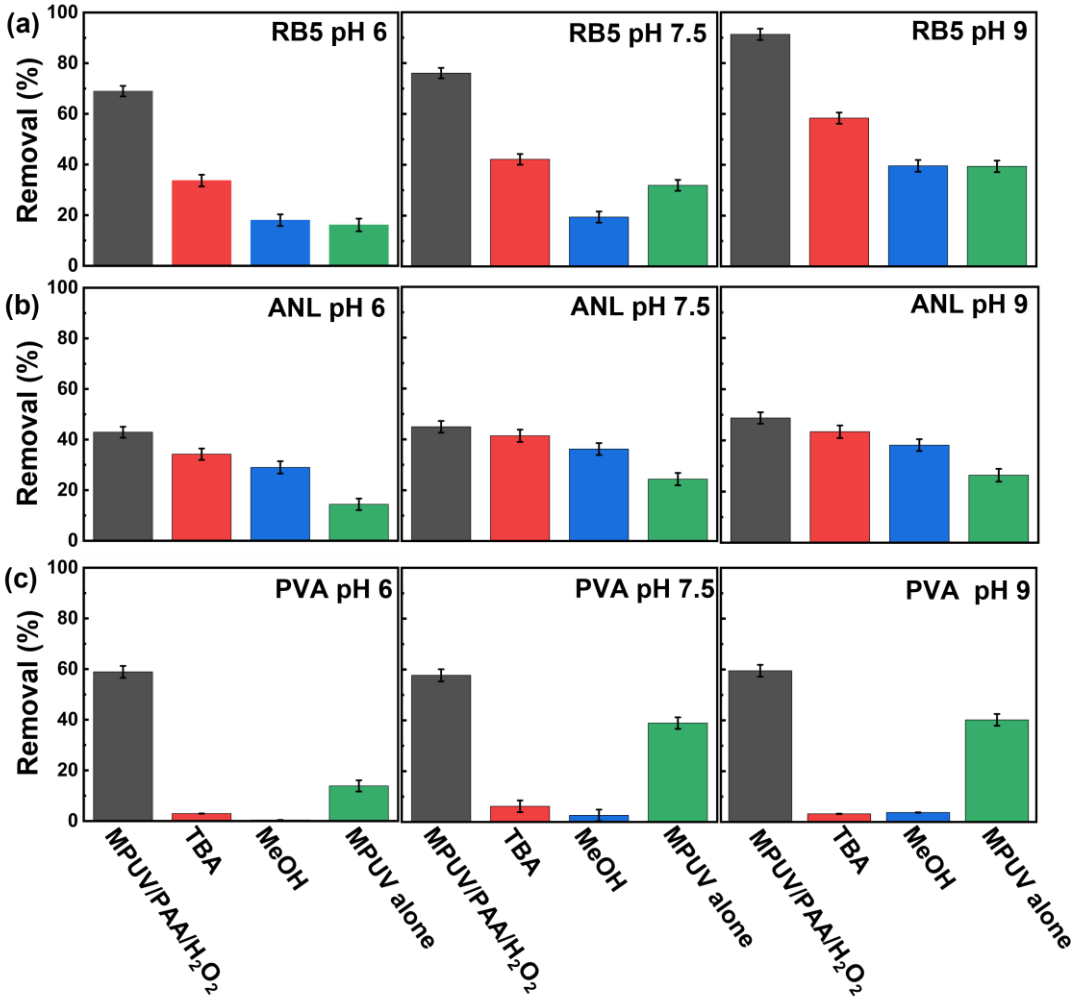

Figure 3. Removal rates of (**a**) RB5, (**b**) ANL, and (**c**) PVA in MPUV/PAA/H_2O_2, MPUV/PAA/H_2O_2 + TBA, MPUV/PAA/H_2O_2 + MeOH, and MPUV only systems at pH 6, 7.5, and 9, respectively. Conditions: $[\text{Contaminant}]_0$ = 10 mg/L, $[\text{PAA}]_0$ = 15 mg/L, $[H_2O_2]_0$ = 3 mg/L, UV fluence rate = 5 mW/cm^2, UV exposure time = 5 min, T = 25 ± 1 °C.

As for ANL, neither TBA nor MeOH addition resulted in a significant decrease in its removal, indicating minor contributions of radicals. The UV-induced removal increased from 14.4% to 24.4% and 24.4% as pH increased from 6 to 7.5 and 9, with the relative contributions increased from 33.6% to 54.2% and 54.1%. These results indicated that PAA oxidation probably played a key role, as well as UV photolysis, in its removal.

Comparatively, the addition of TBA and MeOH resulted in similar quenching effects on PVA removal, implying that •OH played an important role in PVA removal instead of R-C•. Besides, contributions of UV irradiation were 13.9%, 38.9%, and 40.2% at pH 6, 7.5, and 9. These results indicated that •OH oxidation and UV photolysis were the dominant mechanisms relevant to PVA degradation.

3.4. Effect of Coexisting Substances on MPUV/PAA Degradation of Target Pollutants

Considering that textile wastewater generally has high contents of SO_4^{2-} and Cl^- [55], their effects on the removal of RB5, ANL, and PVA in the MPUV/PAA/H_2O_2 system were investigated with the anions' concentrations of 0–2000 mg/L. As shown in Figure 4a–c, the coexistence of SO_4^{2-} had no effect on their removal rates. Figure 4d–f suggested that the coexisting Cl^- had no effect on the removal of RB5 and ANL, but decreased the removal of PVA from 59.5% to 50.6% when the Cl^- dosage increased from 0 to 2000 mg/L. Such an

inhibition effect of PVA removal at a high concentration of Cl^- was probably because Cl^- reacted with •OH to generate Cl•, HOCl•, and Cl_2• [56].

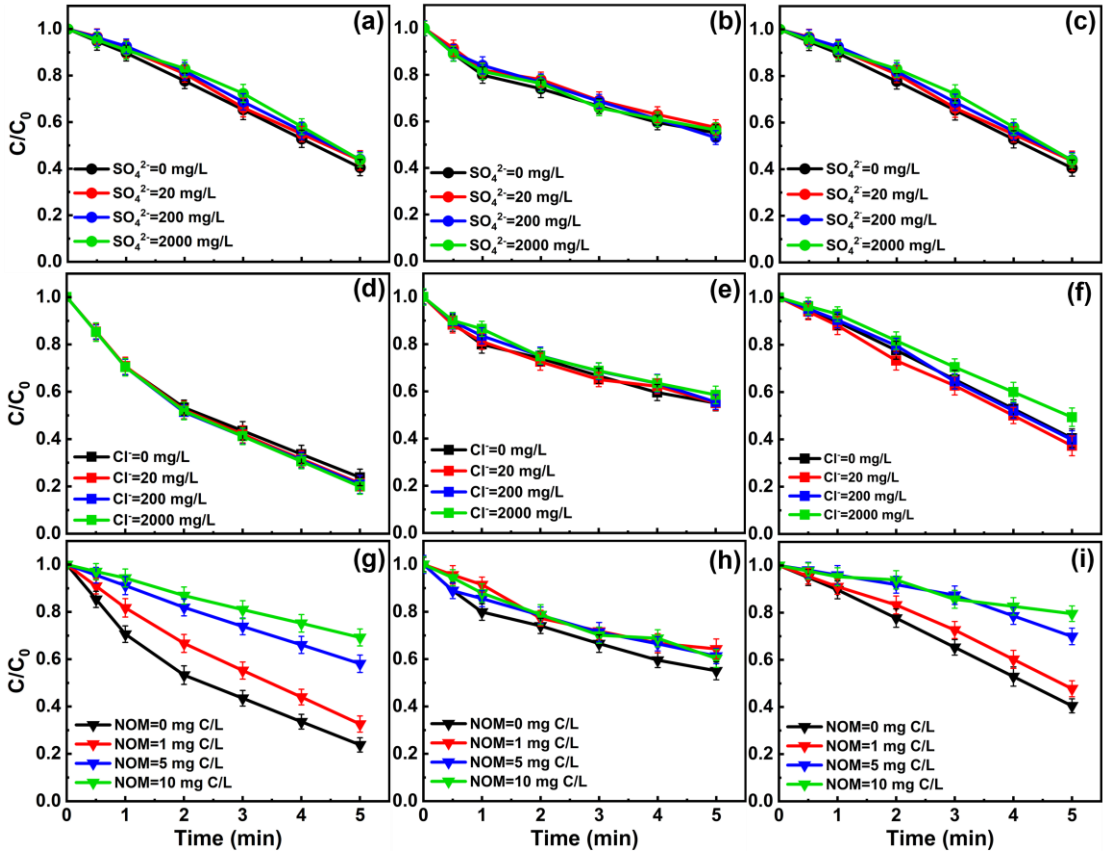

Figure 4. Effect of coexisting SO_4^{2-}, Cl^-, and NOM on the degradation of (**a**,**d**,**g**) RB5, (**b**,**e**,**h**) ANL, and (**c**,**f**,**i**) PVA in the MPUV/PAA system. Conditions: $[PAA]_0$ = 15 mg/L, $[Contaminant]_0$ = 10 mg/L, pH = 7.5, T = 25 ± 1 °C, UV exposure time = 5 min.

Besides, the effect of NOM, represented by natural fulvic acid (FA) [57], on their removal rates was investigated. Figure 4g–i showed that, with the increasing FA concentration from 0 to 10 mg C/L, the removal of RB5 and PVA decreased from 75 to 30.80% and from 51.44 to 33.43%, respectively. The inhibition mechanisms may include: (1) FA contained a large number of unsaturated groups and could absorb a part of photons, resulting in a lower absorption of photons by PAA [58], and (2) FA acted as a quencher of •OH and R-C• [59]. Relatively, the coexisting FA showed a tiny influence on ANL, probably because •OH and R-C• were not the dominant reason for the removal.

3.5. Degradation Performance of MPUV/PAA in Real Water Bodies

The effectiveness of the MPUV/PAA/H_2O_2 system was investigated in removing the three target pollutants in secondary sedimentation effluent of a wastewater plant (pH = 6.8). As shown in Figure 5, the removal rates of RB5, ANL, and PVA in real water were 80.54, 56.26, and 39.83%, respectively. The removal of RB5 or ANL in real water was almost the same as that in the buffer solution, while PVA removal in the former was relatively lower compared with the latter, probably because of the competing effect of DOM in real water based on the reported high reaction rates between DOM with •OH [60]. This result proved the feasibility of MPUV/PAA/H_2O_2 to remove RB5, ANL, and PVA to different extents in real water.

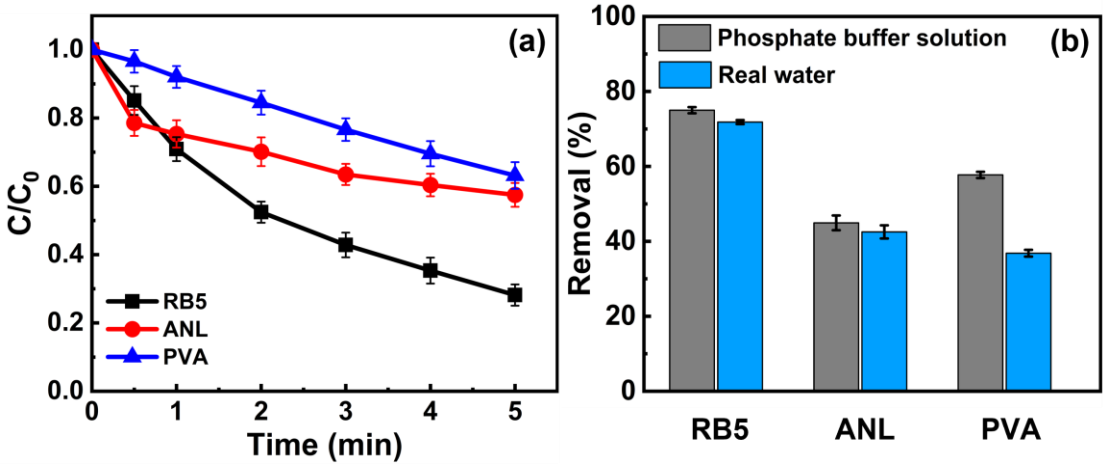

Figure 5. (**a**) Removal of the three pollutants in real water with time. (**b**) Removal comparison in the real water and phosphate buffer solution. Conditions: $[PAA]_0$ = 15 mg/L, $[Contaminant]_0$ = 10 mg/L, pH = 7.5, T = 25 ± 1 °C, UV exposure time = 5 min.

3.6. Acute Toxicity Evaluation

A bioluminescent bacteria test was used to evaluate the acute toxicity of different systems. Figure 6 shows that RB5 had an inhibition rate of around 21% on luminescent bacteria. After treating with PAA, MPUV/PAA/H_2O_2, and MPUV/H_2O_2, the inhibition rates significantly decreased, especially the latter, which was consistent with previously reported toxicity results in Fe^{2+}/PAA/H_2O_2 and Fe^{2+}/H_2O_2 treatments [61]. Compared with RB5, PVA showed a lower inhibition rate (12%), which greatly decreased after the three treatments. Interestingly, ANL had the lowest inhibition rate, which increased after treatment with MPUV/H_2O_2, indicating the likely formation of toxic products induced by •OH oxidation [62]. In conclusion, MPUV/PAA/H_2O_2 treatment could effectively degrade the three target pollutants without causing more toxicity.

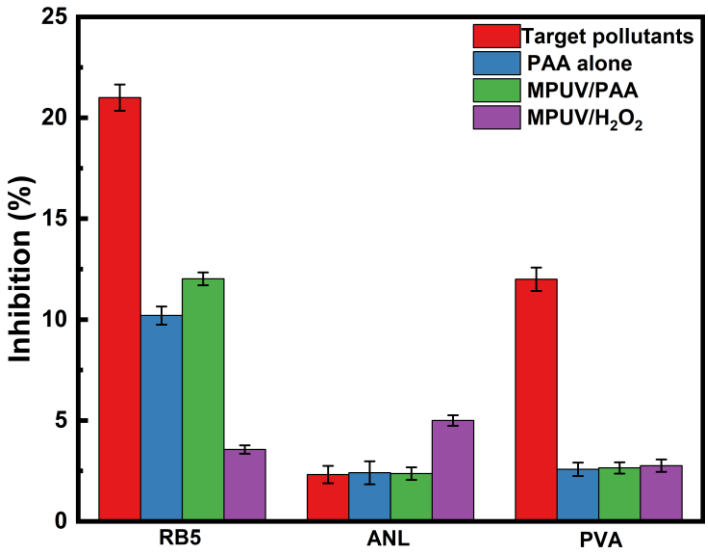

Figure 6. Acute toxicity changes of RB5, ANL, and PVA before and after degradation. Conditions: $[PAA]_0$ = 15 mg/L, $[H_2O_2]_0$ = 3 mg/L, $[Contaminant]_0$ = 10 mg/L, pH = 7.5, T = 25 ± 1 °C, UV exposure time = 5 min.

4. Conclusions

During the treatment with MPUV/PAA/H_2O_2 for 5 min, RB5, ANL, and PVA showed removal rates of 75.0, 44.9, and 57.7%, respectively. Oxidation of PAA and the derived

R-C• showed high selectivity to aromatic organics such as ANL and RB5. The removal of RB5 increased from 68.98 to 91.2%, with pH increasing from 6 to 9, while the removal rates of ANL and PVA were less pH-dependent, in the ranges of 42.9–48.7% and 57–58%, respectively. Quenching experiment results indicated that both •OH and R-C• oxidation contributed to RB5 removal, PAA oxidation played a key role in ANL removal, while •OH oxidation mainly functioned in PVA removal. The coexistence of NOM showed a negative influence on the removal rates of RB5 and PVA. In addition, MPUV/PAA/H_2O_2 treatment could effectively degrade the three target pollutants without causing more toxicity. The results indicated the necessity to evaluate the selective activity of MPUV/PAA/H_2O_2 towards structurally different contaminants before its application in treating printing and dyeing wastewater.

Author Contributions: Methodology, H.X.; Formal analysis, Y.Z. and Y.C.; Resources, P.Z.; Writing—original draft, Y.Z. and Y.C.; Writing—review & editing, Y.Z.; Supervision, D.C.; Project administration, D.W.; Funding acquisition, S.S. All authors have read and agreed to the published version of the manuscript.

Funding: This work was supported by the National Natural Science Foundation of China (No. 52000023), the Shanghai Committee of Science and Technology (No. 19DZ1204400), the Fundamental Research Funds for the Central Universities (22D111317), the Key R&D Program of Guangdong Province (2020B0202010005), the Science and Technology Service Program of Chinese Academy of Science (KFJ-STS-QYZD-199), the Key R&D Program of Inner Mongolia Autonomous Region (2021GG0300), and the National Natural Science Foundation of China (52000025).

Data Availability Statement: All data supporting this study are available in the supplementary information accompanying this paper.

Conflicts of Interest: The authors declare no conflict of interest.

References

1. Méndez-Martínez, A.J.; Dávila-Jiménez, M.M.; Ornelas-Dávila, O.; Elizalde-González, M.P.; Arroyo-Abad, U.; Sirés, I.; Brillas, E. Electrochemical reduction and oxidation pathways for reactive black 5 dye using nickel electrodes in divided and undivided cells. *Electrochim. Acta* **2012**, *59*, 140–149. [CrossRef]
2. Zhang, Y.; Teng, J.; Zhang, X. Research progress on printing and dyeing wastewater treatment technology. *Guangdong Chem. Ind.* **2010**, *37*, 217–218.
3. Kishor, R.; Purchase, D.; Saratale, G.D.; Ferreira, L.F.R.; Bilal, M.; Chandra, R.; Bharagava, R.N. Ecotoxicological and health concerns of persistent coloring pollutants of textile industry wastewater and treatment approaches for environmental safety. *J. Environ. Chem. Eng.* **2021**, *9*, 105012. [CrossRef]
4. Ren, S.; Liu, D.; Chen, Y.; An, S.; Zhao, Y.; Zhang, Y. Anionic channel membrane encircled by SO_3H-polyamide 6 particles for removal of anionic dyes. *J. Membr. Sci.* **2019**, *570*, 34–43. [CrossRef]
5. Rafatullah, M.; Sulaiman, O.; Hashim, R.; Ahmad, A. Adsorption of methylene blue on low-cost adsorbents: A review. *J. Hazard. Mater.* **2010**, *177*, 70–80. [CrossRef]
6. Zhu, M.-X.; Lee, L.; Wang, H.-H.; Wang, Z. Removal of an anionic dye by adsorption/precipitation processes using alkaline white mud. *J. Hazard. Mater.* **2007**, *149*, 735–741. [CrossRef]
7. Ibrahim, S.M.; Badawy, A.A.; Essawy, H.A. Improvement of dyes removal from aqueous solution by Nanosized cobalt ferrite treated with humic acid during coprecipitation. *J. Nanostruct. Chem.* **2019**, *9*, 281–298. [CrossRef]
8. Lau, Y.; Wong, Y.; Teng, T.; Morad, N.; Rafatullah, M.; Ong, S.-A. Degradation of cationic and anionic dyes in coagulation–flocculation process using bi-functionalized silica hybrid with aluminum-ferric as auxiliary agent. *RSC Adv.* **2015**, *5*, 34206–34215. [CrossRef]
9. Moghaddam, S.S.; Moghaddam, M.A.; Arami, M. Coagulation/flocculation process for dye removal using sludge from water treatment plant: Optimization through response surface methodology. *J. Hazard. Mater.* **2010**, *175*, 651–657. [CrossRef]
10. Javaid, R.; Qazi, U.Y. Catalytic oxidation process for the degradation of synthetic dyes: An overview. *Int. J. Environ. Res. Public Health* **2019**, *16*, 2066. [CrossRef]
11. Zaharia, C.; Suteu, D.; Muresan, A.; Muresan, R.; Popescu, A. Textile wastewater treatment by homogenous oxidation with hydrogen peroxide. *Environ. Eng. Manag. J.* **2009**, *8*, 1359–1369. [CrossRef]
12. Cheng, L.; Wei, M.; Huang, L.; Pan, F.; Xia, D.; Li, X.; Xu, A. Efficient H_2O_2 oxidation of organic dyes catalyzed by simple copper (II) ions in bicarbonate aqueous solution. *Ind. Eng. Chem. Res.* **2014**, *53*, 3478–3485. [CrossRef]
13. Bhatia, D.; Sharma, N.R.; Singh, J.; Kanwar, R.S. Biological methods for textile dye removal from wastewater: A review. *Crit. Rev. Environ. Sci. Technol.* **2017**, *47*, 1836–1876. [CrossRef]

14. Araghi, M.S.; Olya, M.E.; Marandi, R.; Siadat, S.D. Investigation of enhanced biological dye removal of colored wastewater in a lab-scale biological activated carbon process. *Appl. Biol. Chem.* **2016**, *59*, 463–470. [CrossRef]
15. Amini, M.; Arami, M.; Mahmoodi, N.M.; Akbari, A. Dye removal from colored textile wastewater using acrylic grafted nanomembrane. *Desalination* **2011**, *267*, 107–113. [CrossRef]
16. Nguyen, T.A.; Juang, R.-S. Treatment of waters and wastewaters containing sulfur dyes: A review. *Chem. Eng. J.* **2013**, *219*, 109–117. [CrossRef]
17. Dasgupta, J.; Sikder, J.; Chakraborty, S.; Curcio, S.; Drioli, E. Remediation of textile effluents by membrane based treatment techniques: A state of the art review. *J. Environ. Manag.* **2015**, *147*, 55–72. [CrossRef]
18. Man, X.; Ning, X.A.; Lu, X.; Liang, J.; Liu, D.; Lai, X. Degradation of polycyclic aromatic hydrocarbons from textile dyeing sludge by ultrasound/Fe~0/EDTA system. *Acta Sci. Circumst.* **2018**, *38*, 1049–1055.
19. Anan, D.; Yanlei, S.; Wenjuan, C.; Peng, J.; Zhang, Y.; Jiang, Z. Ultrafiltration enhanced with activated carbon adsorption for efficient dye removal from aqueous solution. *Chin. J. Chem. Eng.* **2011**, *19*, 863–869.
20. Lucas, M.S.; Peres, J.A. Decolorization of the azo dye Reactive Black 5 by Fenton and photo-Fenton oxidation. *Dyes Pigments* **2006**, *71*, 236–244. [CrossRef]
21. Tehrani-Bagha, A.; Mahmoodi, N.M.; Menger, F. Degradation of a persistent organic dye from colored textile wastewater by ozonation. *Desalination* **2010**, *260*, 34–38. [CrossRef]
22. Hou, L.; Wu, Q.; Gu, Q.; Zhou, Q.; Zhang, J. Community structure analysis and biodegradation potential of aniline-degrading bacteria in biofilters. *Curr. Microbiol.* **2018**, *75*, 918–924. [CrossRef]
23. Miralles-Cuevas, S.; Oller, I.; Agüera, A.; Llorca, M.; Pérez, J.S.; Malato, S. Combination of nanofiltration and ozonation for the remediation of real municipal wastewater effluents: Acute and chronic toxicity assessment. *J. Hazard. Mater.* **2017**, *323*, 442–451. [CrossRef] [PubMed]
24. Sun, W.; Chen, L.; Wang, J. Degradation of PVA (polyvinyl alcohol) in wastewater by advanced oxidation processes. *J. Adv. Oxid. Technol.* **2017**, *20*, 20170018. [CrossRef]
25. Cheng, C.; Li, H.D.; Wang, J.L.; Wang, H.L.; Yang, X.J. A review of measurement methods for peracetic acid (PAA). *Front. Environ. Sci. Eng.* **2020**, *14*, 87. [CrossRef]
26. Ketel, D.H. Distribution and accumulation of thiophenes in plants and calli of different Tagetes species. *J. Exp. Bot.* **1987**, *38*, 322–330. [CrossRef]
27. Ao, X.W.; Eloranta, J.; Huang, C.H.; Santoro, D.; Sun, W.J.; Lu, Z.D.; Li, C. Peracetic acid-based advanced oxidation processes for decontamination and disinfection of water: A review. *Water Res.* **2021**, *188*, 116479. [CrossRef]
28. Sharma, S.; Mukhopadhyay, M.; Murthy, Z.V.P. UV/peroxyacetic acid mediated chlorophenol congener degradation. *CLEAN–Soil Air Water* **2014**, *42*, 276–283. [CrossRef]
29. Cai, M.; Sun, P.; Zhang, L.; Huang, C.H. UV/peracetic acid for degradation of pharmaceuticals and reactive species evaluation. *Environ. Sci. Technol.* **2017**, *51*, 14217–14224. [CrossRef]
30. Zhang, L.; Liu, Y.Q.; Fu, Y.S. Degradation kinetics and mechanism of diclofenac by UV/peracetic acid. *RSC Adv.* **2020**, *10*, 9907–9916. [CrossRef]
31. Araujo, F.V.D.; Yokoyama, L.; Teixeira, L.A.C. Color removal in reactive dye solutions by UV/H_2O_2 oxidation. *Quim. Nova* **2006**, *29*, 11–14. [CrossRef]
32. Xue, G.; Zheng, M.H.; Qian, Y.J.; Li, Q.; Gao, P.; Liu, Z.; Chen, H.; Li, X. Comparison of aniline removal by UV/CaO_2 and UV/H_2O_2: Degradation kinetics and mechanism. *Chemosphere* **2020**, *255*, 126983. [CrossRef] [PubMed]
33. Lin, C.C.; Lee, L.T. Degradation of polyvinyl alcohol in aqueous solutions using UV/oxidant process. *J. Ind. Eng. Chem.* **2015**, *21*, 569–574. [CrossRef]
34. Chen, S.; Cai, M.Q.; Liu, Y.Z.; Zhang, L.Q. Effects of water matrices on the degradation of naproxen by reactive radicals in the UV/peracetic acid process. *Water Res.* **2019**, *150*, 153–161. [CrossRef] [PubMed]
35. Xingzu, W.; Cheng, X.; Dezhi, S.; Qi, H. Biodecolorization and partial mineralization of reactive black 5 by a strain of Rhodopseudomonas palustris. *J. Environ. Sci.* **2008**, *20*, 1218–1225.
36. Zhang, S.J.; Yu, H.Q. Radiation-induced degradation of polyvinyl alcohol in aqueous solutions. *Water Res.* **2004**, *38*, 309–316. [CrossRef]
37. Xiao, J.; Wang, M.; Pang, Z.; Dai, L.; Lu, J.; Zou, J. Simultaneous spectrophotometric determination of peracetic acid and the coexistent hydrogen peroxide using potassium iodide as the indicator. *Anal. Methods* **2019**, *11*, 1930–1938. [CrossRef]
38. Liu, B.; Guo, W.; Wang, H.; Si, Q.; Zhao, Q.; Luo, H.; Ren, N. Activation of peroxymonosulfate by cobalt-impregnated biochar for atrazine degradation: The pivotal roles of persistent free radicals and ecotoxicity assessment. *J. Hazard. Mater.* **2020**, *398*, 122768. [CrossRef]
39. Su, C.C.; Pagaling, E.D.; Peralta, G.L.; Lu, M.-C. Comparison of Aniline Degradation by Fenton and Electro-Fenton Reactors Using Plate and Rod Electrodes. *Environ. Prog. Sustain. Energy* **2014**, *33*, 410–418. [CrossRef]
40. Du, P.; Liu, W.; Cao, H.; Zhao, H.; Huang, C.-H. Oxidation of amino acids by peracetic acid: Reaction kinetics, pathways and theoretical calculations. *Water Res. X* **2018**, *1*, 100002. [CrossRef]
41. Zhang, K.; Zhou, X.; Du, P.; Zhang, T.; Cai, M.; Sun, P.; Huang, C.-H. Oxidation of β-lactam antibiotics by peracetic acid: Reaction kinetics, product and pathway evaluation. *Water Res.* **2017**, *123*, 153–161. [CrossRef] [PubMed]
42. Kim, J.; Huang, C.H. Reactivity of peracetic acid with organic compounds: A critical review. *ACS ES&T Water* **2020**, *1*, 15–33.

43. Sun, P.; Zhang, T.; Mejia-Tickner, B.; Zhang, R.; Cai, M.; Huang, C.-H. Rapid Disinfection by Peracetic acid combined with UV Irradiation. *Environ. Sci. Technol. Lett.* **2018**, *5*, 400–404. [CrossRef]
44. Hollman, J.; Dominic, J.A.; Achari, G. Degradation of pharmaceutical mixtures in aqueous solutions using UV/peracetic acid process: Kinetics, degradation pathways and comparison with UV/H_2O_2. *Chemosphere* **2020**, *248*, 125911. [CrossRef] [PubMed]
45. Zhang, T.Q.; Huang, C.H. Modeling the Kinetics of UV/Peracetic acid Advanced Oxidation Process. *Environ. Sci. Technol.* **2020**, *54*, 7579–7590. [CrossRef]
46. Hamad, D.; Mehrvar, M.; Dhib, R. Experimental study of polyvinyl alcohol degradation in aqueous solution by UV/H_2O_2 process. *Polym. Degrad. Stab.* **2014**, *103*, 75–82. [CrossRef]
47. Liang, H.; Chen, Z.M.; Huang, D.; Zhao, Y.; Li, Z.Y. Impacts of aerosols on the chemistry of atmospheric trace gases: A case study of peroxides and HO_2 radicals. *Atmos. Chem. Phys.* **2013**, *13*, 11259–11276. [CrossRef]
48. Gao, J.; Luo, C.W.; Gan, L.; Wu, D.J.; Tan, F.X.; Cheng, X.X.; Zhou, W.W.; Wang, S.S.; Zhang, F.M.; Ma, J. A comparative study of UV/H_2O_2 and UV/PDS for the degradation of micro-pollutants: Kinetics and effect of water matrix. *Environ. Sci. Pollut. Res.* **2020**, *27*, 24531–24541. [CrossRef]
49. Chen, Z.; Liu, Y.; Fu, Y. Photochemical Degradation of triclosan by Ultraviolet-Peracetic acid. *Technol. Water Treat.* **2021**, *47*, 36.
50. Joseph, C.G.; Taufiq-Yap, Y.H.; Krishnan, V. Ultrasonic assisted photolytic degradation of reactive black 5 (RB5) simulated wastewater. *ASEAN J. Chem. Eng.* **2017**, *17*, 37–50. [CrossRef]
51. Kunz, A.; Mansilla, H.; Duran, N. A degradation and toxicity study of three textile reactive dyes by ozone. *Environ. Technol.* **2002**, *23*, 911–918. [CrossRef]
52. Anipsitakis, G.P.; Dionysiou, D.D. Radical generation by the interaction of transition metals with common oxidants. *Environ. Sci. Technol.* **2004**, *38*, 3705–3712. [CrossRef] [PubMed]
53. Grosjean, D.; Williams, E.L., II. Environmental persistence of organic compounds estimated from structure-reactivity and linear free-energy relationships. Unsaturated aliphatics. *Atmos. Environ. Part A* **1992**, *26*, 1395–1405. [CrossRef]
54. Kim, J.; Du, P.; Liu, W.; Luo, C.; Zhao, H.; Huang, C.H. Cobalt/peracetic acid: Advanced oxidation of aromatic organic compounds by acetylperoxyl radicals. *Environ. Sci. Technol.* **2020**, *54*, 5268–5278. [CrossRef] [PubMed]
55. Zhou, C.; Li, C.; Yang, K.; Hu, Y.; Xu, X. Sb(V)removal by different iron oxides from simulated textile-wastewater. *Acta Sci. Circumst.* **2022**, *42*, 96–107.
56. Li, L.; Huang, J.; Hu, X.; Zhang, S.; Dai, Q.; Chai, H.; Gu, L. Activation of sodium percarbonate by vanadium for the degradation of aniline in water: Mechanism and identification of reactive species. *Chemosphere* **2019**, *215*, 647–656. [CrossRef]
57. Liu, Y.L.; Li, C.; Lou, Z.M.; Zhou, C.C.; Yang, K.L.; Xu, X.H. Antimony removal from textile wastewater by combining PFS&PAC coagulation: Enhanced Sb(V) removal with presence of dispersive dye. *Sep. Purif. Technol.* **2021**, *275*, 119037.
58. Luo, X.; Zheng, Z.; Greaves, J.; Cooper, W.J.; Song, W. Trimethoprim: Kinetic and mechanistic considerations in photochemical environmental fate and AOP treatment. *Water Res.* **2012**, *46*, 1327–1336. [CrossRef] [PubMed]
59. Luo, C.; Ma, J.; Jiang, J.; Liu, Y.; Song, Y.; Yang, Y.; Guan, Y.; Wu, D. Simulation and comparative study on the oxidation kinetics of atrazine by UV/H_2O_2, UV/HSO_5^- and UV/$S_2O_8^{2-}$. *Water Res.* **2015**, *80*, 99–108. [CrossRef]
60. Li, N.; Qiao, X.; Uiu, Y.; Fei, Z. Oxidization of dissolved organic matters from different sources by hydroxyl radical. *Environ. Chem.* **2015**, *34*, 1246–1251.
61. Yu, J.L.; Shu, S.H.; Wang, Q.F.; Gao, N.Y.; Zhu, Y.P. Evaluation of Fe^{2+}/Peracetic acid to degrade three typical refractory pollutants of textile wastewater. *Catalysts* **2022**, *12*, 684. [CrossRef]
62. Prasse, C.; Ford, B.; Nomura, D.K.; Sedlak, D.L. Unexpected transformation of dissolved phenols to toxic dicarbonyls by hydroxyl radicals and UV light. *Proc. Natl. Acad. Sci. USA* **2018**, *115*, 2311–2316. [CrossRef] [PubMed]